Application of Feedback Linearization in Adaptive Controller Design

Arijit Ganguly, Anik Sarkar, Arnab Ghosh, Parijat Bhowmick, and Sawan Sen

Abstract This paper presents a method to convert the non-linear dynamics of a system into their reformulated linearized forms using feedback linearization. The proposed technique allows to transform the non-linear model of a system into a *n*th order integrator form whose performance can be controlled. The process of feedback linearization has been applied to non-linear models of dispersed generator (DG) units and robotic agents to design an adaptive secondary control scheme for an AC microgrid disconnected to the main grid and a team of robotic agents, respectively. A detailed case study with a deep simulation has been done to confirm the effectiveness of the linearization technique and the adaptive control scheme. A comparative analysis has been also done between the proposed adaptive control scheme and the conventional cooperative control scheme for DG-based islanded AC microgrid to further demonstrate the effectiveness of adaptive design of the controller.

Keywords Non-linear systems · Linearized models · Feedback linearization · Adaptive controller · Islanded AC microgrid · Robotic agents

---

A. Ganguly (✉)
Department of Computer Science Engineering, Institute of Engineering and Management, University of Engineering and Management, Kolkata, West Bengal, India
e-mail: arijit.ganguly@uem.edu.in

A. Sarkar · S. Sen
Electrical Electrical Department, Kalyani Government Engineering College, Kalyani, Nadia, West Bengal, India

A. Ghosh
Department of Electrical Engineering, Institute of Engineering and Management, University of Engineering and Management, Kolkata, West Bengal, India
e-mail: arnab.ghosh1@uem.edu.in

P. Bhowmick
Department of Electronics and Electrical Engineering, IIT Guwahati, Guwahati, Assam, India
e-mail: parijat.bhowmick@iitg.ac.in

M. Pal et al. (eds.), *Innovations in Energy Management and Renewable Resources*,
Lecture Notes in Electrical Engineering 1239,
https://doi.org/10.1007/978-981-97-6390-0_10

1 Introduction

The successful design of a controller depends on the nature and type of a system to a great extent. The conventional controller synthesis techniques and system stability analysis methodologies following graphical methods (root locus), lag lead compensator design using bode plot or Nyquist plot, PID controller design via Ziegler-Nichols, Cohen-coon, etc., tuning algorithms, Kharitoniv's theorem, finding eigenvalues of the system, state feedback control via pole-placement holds good for linear time invariant systems [1]. Hence, the stability analysis of a system and the controller synthesis can be implemented using the above-mentioned classical and modern control schemes.

The design of controller for analyzing the performance of non-linear systems and ensuring their asymptotic stability faces a multitude of problems in terms of reference tracking, steady state error minimization and meeting the desired time domain specifications [2]. In [3], cooperative control design of multi-missile system has been shown where missiles are represented by their linearized forms. Li et al. [4] discuss about the optimal cooperative controller design for multi-agent systems over fixed communication network topology. In [5], cooperative control scheme for multi-vehicle systems are discussed where the vehicular systems are represented by their linearized models. This necessitates the transformation of non-linear models of a system into their controllable reformulated linearized dynamics [6–8] so that the classical and modern control schemes can be applied for the synthesis of controller.

In this work, the non-linear models of a system have been transformed into linearized controllable single and double integrator systems using feedback linearization. The concept of feedback linearization enables the application of an adaptive control scheme for the design of secondary controller in a DG-based islanded AC microgrid [9–12]. The DGs in an islanded AC microgrid are considered to be homogeneous systems having similar non-linear dynamics. The adaptive secondary controller design comprises of secondary voltage and frequency control action. Using feedback linearization, the DGs in an islanded AC microgrid are modeled as double integrator agents for secondary voltage control and as single integrator agents for secondary frequency control action.

The non-linear models of robotic agents working in a team have been also linearized to double integrator systems using feedback linearization. A cooperative control scheme has been designed to achieve a common target by this team of robotic agents.

A cooperative control framework in a multi-agent system provides a rapid coordination and agreement among the agents [13–17]. Each agent exchanges their state information to their neighboring agents via communication network [18]. Cooperative control can be classified as a design to achieve formation control and consensus. Consensus can be further classified as leaderless consensus and leader following consensus. In case of leaderless consensus scheme, a particular state is formed by calculating the average of the initial states of all the participating agents present in multi-agent network. The controller design forces the state of all agents to reach the

Table 1 Notation

Microgrid parameters symbol	Corresponding meaning
ω_i	Angular frequency of the ith DG
ω_{com}	Rotating reference frequency
ϕ_i	Angle of the ith DG reference frame
α_i , β_i	Measured active and reactive power at the DG terminal
m_{α_i} , n_{β_i}	Droop coefficients
ω_{n_i} , v_{n_i}	Primary control references
$I^{\star}_{ld_i}$, $I^{\star}_{lq_i}$, $V^{\star}_{2d_i}$, $V^{\star}_{2q_i}$	Current and voltage controller references
V_{2_i} and I_{2_i}	Power controller reference
ψ_{d_i} , ψ_{q_i} , λ_{d_i} and λ_{q_i}	Auxiliary state variables for the voltage and current controllers
ω_{c_i}	Cut-off frequency of the low-pass filters
ω_b	Nominal angular frequency
K_{1_i} , K_{2_i} , K_{3_i} and K_{4_i}	PI type controller gains of both the voltage and current controllers, respectively
R_{1_i} , C_{1_i} , L_{1_i}	Output filter parameters
R_{2_i} , L_{2_i}	Output connector parameters
V_{bsd_i} , V_{bsq_i}	Bus voltages of ith DG along d-q axis
$V_{l_{i}d_i}$, $V_{l_{i}q_i}$	Line voltages of ith DG along d-q axis
Robot parameters symbol	Corresponding meaning
ω_{r_i}	Angular velocity of ith robot
θ_{r_i}	Heading angle of the ith robot
v_{r_i}	Linear velocity of the ith robot
$u_{r_{yi}}$	Feedback linearized control input along y-axis
$u_{r_{xi}}$	Feedback linearized control input along x-axis
u_{r_i}	Feedback linearized control input
$v_{r_{yi}}$	Linear velocity component along Y-axis
$v_{r_{xi}}$	Linear velocity component along X-axis

calculated average of all initial states. The leader following consensus scheme (see Fig. 1) drives the states of all participating agents in multi-agent network towards the state of leader.

The controller design requires the coupling gain, formation control vector, the state feedback gain and the cooperative tracking error formed by the elements of adjacency matrix and exchange of state information. Table 1 describes the notations used in the work.

The main objective of the work has been outlined as follows:

(i) Convert the non-linear dynamics of a system to its linearized controllable form using feedback linearization so that feedback control laws can be applied.

(ii) Apply feedback linearization upon non-linear DG models and then design an adaptive control scheme in a DG-based islanded AC microgrid.

(iii) Use feedback linearization as a tool to linearize non-linear robot models, which is required to design an adaptive control scheme for a team of two-wheel mobile robots working in a mission.

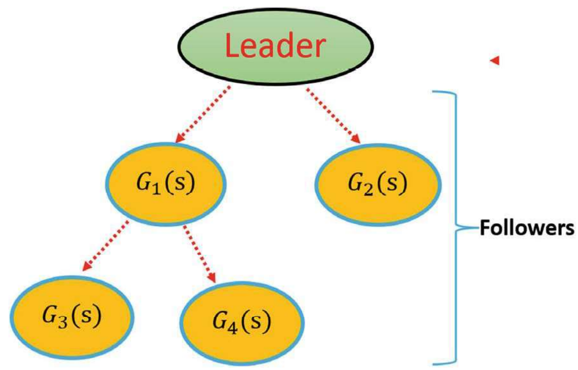

Fig. 1 Leader following multiple agents in a distributed network

2 Technical Background and Essential Preliminaries

2.1 Feedback Linearization

The principle idea is to transform a non-linear system into a fully or partially linearized system so that the feedback control laws could be applied. Feedback linearization can be classified as input-state linearization and input-output linearization. In input-state linearization, the full state equation is linearized and in input-output linearization, the output equation is linearized and is explicitly expressed in terms of the control input. Here, the state equation may or may not be linearized.

Consider the state equation

$$\begin{cases} \dot{x} = f(x) + g(x)u \\ y = h(x) \end{cases} \tag{1}$$

In input-state linearization, the goal is to cancel out the non-linearities in $f(x)$ and $g(x)$ and in input-output linearization, the goal is to cancel out the non-linearities in $h(x)$.

2.2 Control Scheme

This paper mainly discusses the leader following consensus scheme to design the adaptive controller. The controller operates to drive the voltages and frequencies of the microgrid DG units to reach the consensus value. The consensus value is considered as reference in the network. In case of networked robotic agents, the cooperative controller performs its operation to make the robots move towards a targeted object and the targeted object is considered as the leader.

2.3 DG-Based Islanded AC Microgrid

The DG units of the islanded AC microgrid are characterized by a set of governing differential-algebraic equations (DAEs), which are given by:

$$\begin{cases} \omega_i = \omega_{n_i} - m_{\alpha_i}\alpha_i \\ v^{\star}_{2,mag_i} = \nu_{n_i} - n_{\beta_i}\beta_i \\ \dot{\phi}_i = \omega_i - \omega_{\text{com}} \end{cases} \tag{2}$$

The dynamical equations of the power controller are given by:

$$\begin{cases} \dot{\alpha}_i = -\omega_{c_i}\alpha_i + \omega_{c_i}\left(V_{2d_i}I_{2d_i} + V_{2q_i}I_{2q_i}\right) \\ \dot{\beta}_i = -\omega_{c_i}\beta_i + \omega_{c_i}\left(V_{2q_i}I_{2d_i} - V_{2d_i}I_{2q_i}\right) \end{cases} \tag{3}$$

The dynamical equations of the voltage controller are given by:

$$\begin{cases} I^{\star}_{ld_i} = \eta_i I_{2d_i} - \omega_b C_{1_i} V_{2q_i} + K_{1_i}(V^{\star}_{2d_i} - V_{2d_i}) + K_{2_i}\psi_{d_i} \\ I^{\star}_{lq_i} = \eta_i I_{2q_i} - \omega_b C_{1_i} V_{2d_i} + K_{1_i}(V^{\star}_{2q_i} - V_{2q_i}) + K_{2_i}\psi_{q_i} \end{cases} \tag{4}$$

The dynamical equations of the current controller are given by:

$$\begin{cases} V^{\star}_{id_i} = -\omega_b L_{1_i} I_{1q_i} + K_{3_i}\left(I^{\star}_{1d_i} - I_{1d_i}\right) + K_{4_i}\lambda_{d_i} \\ V^{\star}_{iq_i} = \omega_b L_{1_i} I_{1d_i} + K_{3_i}\left(I^{\star}_{1q_i} - I_{1q_i}\right) + K_{4_i}\lambda_{q_i} \end{cases} \tag{5}$$

The dynamical equations of the LC filter present on the output end of DG and the output connector are given by:

$$\begin{cases} \dot{I}_{ld_i} = -\dfrac{R_{1_i}}{L_{1_i}} I_{ld_i} + \omega_i I_{lq_i} + \dfrac{1}{L_{1_i}} V_{l_{id_i}} - \dfrac{1}{L_{1_i}} V_{2d_i}, \\ \dot{I}_{1q_i} = -\dfrac{R_{1_i}}{L_{1_i}} I_{lq_i} - \omega_i I_{ld_i} + \dfrac{1}{L_{1_i}} V_{l_{iq_i}} - \dfrac{1}{L_{1_i}} V_{2q_i}, \\ \dot{V}_{2d_i} = \omega_i V_{2q_i} + \dfrac{1}{C_{1_i}} I_{ld_i} - \dfrac{1}{C_{1_i}} I_{2d_i}, \\ \dot{V}_{2q_i} = -\omega_i V_{2d_i} + \dfrac{1}{C_{1_i}} I_{lq_i} - \dfrac{1}{C_{1_i}} I_{2q_i}, \\ \dot{I}_{2d_i} = -\dfrac{R_{2_i}}{L_{2_i}} I_{2d_i} + \omega_i I_{2q_i} + \dfrac{1}{L_{2_i}} V_{2d_i} - \dfrac{1}{L_{2_i}} V_{bsd_i}, \\ \dot{I}_{2q_i} = -\dfrac{R_{2_i}}{L_{2_i}} I_{2q_i} - \omega_i I_{2d_i} + \dfrac{1}{L_{2_i}} V_{2q_i} - \dfrac{1}{L_{2_i}} V_{bsq_i}. \end{cases} \tag{6}$$

Equations (2–6) suggest us to form the compact state-space model of an inverter-based DG unit, which is expressed as

$$\begin{cases} \dot{\mathbf{x}}_i = \mathbf{g}_i(\mathbf{x}_i) + \mathbf{m}_i(\mathbf{x}_i)\mathbf{W}_i + \mathbf{t}_i(\mathbf{x}_i)u_i \\ y_i = f_i(\mathbf{x}_i) \end{cases} \quad \forall i \in \{1, 2, \ldots, N\} \tag{7}$$

where the expression of the state vector x_i of the ith DG unit is given by $\mathbf{x}_i = \left[\phi_i \ \alpha_i \ \beta_i \ \psi_{d_i} \ \psi_{q_i} \ \lambda_{d_i} \ \lambda_{q_i} \ I_{1d_i} \ I_{1q_i} \ V_{2d_i} \ V_{2q_i} \ I_{2d_i} \ I_{2q_i}\right]^\top$ and $\mathbf{W}_i$ forms a known disturbance.

2.4 Robotic Agents in a Mission

A team of mobile robots connected through a non-varying communication network works in a mission to achieve a particular target. The kinematic equations that describe the two-wheeled mobile robot are given by

$$\left\{ \dot{x}_{xi} = v_{r_i} \cos\theta_{r_i}, \ \dot{x}_{yi} = v_{r_i} \sin\theta_{r_i} \text{ and } \dot{\theta}_{r_i} = \omega_{r_i} \right. \tag{8}$$

for all $i \in \{1, 2, \ldots, n_r\}$ where n_r represents the number of robotic agents present in the team.

3 Main Results

Lemma 1 *Consider a smooth scalar function $h : R^n \rightarrow R$ and a smooth vector field $f : R^n \rightarrow R^n$ on R^n, then the lie derivative of h with respect to f is a scalar function given by $L_f h = \nabla h f$. Lie derivative represents the directional derivative of h along the direction of vector f.*

Lemma 2 *Consider f and g as two vector fields on R^n, then lie bracket of f and g is another vector field defined by $[f, g] = \nabla g f - \nabla f g$.*

Lemma 3 *Relative degree of output refers to the number of times the output is being differentiated so that input explicitly appears in the output. If n is the order of the system and k is the relative degree of output, then*
(i) if $k = n$; system is fully feedback linearizable.
(ii) if $k < n$; system is partially feedback linearizable.

Here the discussion will be restricted to a fully feedback linearizable system.

3.1 Feedback Linearization

This section focuses on input-output feedback linearization since the adaptive controller design of islanded AC microgrid and the cooperative controller design of a team of robotic agents work on linearized systems. This is obtained by applying input-output feedback linearization on the non-linear model of DGs in microgrid and robots in a team of robotic agents. The key idea is to cancel out the non-linearities in the system by choosing an appropriate control input.

Theorem 1 *Using input-output feedback linearization, a non-linear system given by Eq. (1) can be transformed into an equivalent linear system*

$$\begin{cases} \dot{z}_i = Az_i + Bv_i \\ y_{z_i} = Cz_i \end{cases} \quad \forall i \in \{1, 2, \dots n\} \tag{9}$$

Where z_i is the feedback linearized state, y_i is the feedback linearized output and v_i is the auxiliary control input. If there exists a feedback control input $u = \alpha(x) + \beta(x)v$ and a change of state variable $Z = T(x)$ that can transform the non-linear system into an equivalent linear system, then all the classical techniques can be applied to the resulting closed loop system.

Proof Differentiating the output equation present in Eq. (1) with respect to time, we get

$$\dot{y} = \frac{\partial h}{\partial x}\dot{x} \tag{10}$$

Substituting $\dot{x}$ from Eq. (1) in Eq. (10) gives us

$$\dot{y} = \frac{\partial h}{\partial x}(f(x) + g(x)u)$$

Applying Lemma 1, we get

$$\dot{y} = L_f h(x) + L_g h(x)u \tag{11}$$

Since the work moves forward with a fully feedback linearizable system (i.e. k = n), the input should appear explicitly only on the output equation corresponding to the kth derivative. Therefore, the expression $L_g h(x)u$ in Eq. (11) is ignored. Thus, Eq. (11) is reduced to

$$\dot{y} = L_f h(x) \tag{12}$$

Differentiating twice the Eq. (12) gives us

$$y^{(2)} = \frac{\partial L_f h(x)}{\partial x}\dot{x} \tag{13}$$

Substituting $\dot{x}$ from Eq. (1) in Eq. (13) gives us

$$y^{(2)} = \frac{\partial L_f h(x)}{\partial x}(f(x) + g(x)u)$$

Using Lemma 1, we get

$$y^{(2)} = L_f{}^2 h(x) + L_g L_f h(x)u \tag{14}$$

Since still we are moving forward with a fully feedback linearizable system (i.e. k = n), the input should appear explicitly only on the output equation corresponding to the kth derivative. Therefore, the expression $L_g L_f h(x)u$ in Eq. (14) is ignored. If we move up to kth derivative of the output equation, the expression becomes

$$y^{(k)} = L_f{}^k h(x) + L_g L_f^{k-1} h(x)u \tag{15}$$

In Eq. (15), the term $L_g L_f^{k-1} h(x)u$ has to be non-zero as the relative degree of the system is considered as k. The control input u will be chosen in such a way so that it cancels out the non-linearities in Eq. (15). Considering the above statement, control input has been chosen as

$$u = \frac{1}{L_g L_f^{k-1} h(x)}[v - L_f^k h(x)] \tag{16}$$

Substituting u from Eq. (16) to (15), we get,

$$y^k = v \quad or \quad y = \iint \ldots\int v \tag{17}$$

which indicates that output is obtained by k-times integrating v.

Let $\phi_1(x) = y = h(x)$
$\phi_2(x) = \dot{y} = L_f h(x)$
$\phi_3(x) = y^{(2)} = L_f^2 h(x)$
and $\phi_k(x) = y^{(k)} = L_f^{k-1} h(x)$
In matrix form,

$$\phi(x) = \begin{bmatrix} \phi_1(x) \\ \phi_2(x) \\ \phi_3(x) \\ . \\ \phi_k(x) \end{bmatrix} = \begin{bmatrix} h(x) \\ L_f h(x) \\ L_f^2 h(x) \\ . \\ L_f^{k-1} h(x) \end{bmatrix} \tag{18}$$

Let the change of coordinates be

$$z_i = \phi_i(x) = L_f^{i-1} h(x); 1 \le i \le k \tag{19}$$

Hence it can be written as

$$\phi(x) = \begin{bmatrix} \phi_1(x) \\ \phi_2(x) \\ \phi_3(x) \\ . \\ \phi_k(x) \end{bmatrix} = \begin{bmatrix} z_1 \\ z_2 \\ z_3 \\ . \\ z_n \end{bmatrix} \tag{20}$$

Now we get,

$$\begin{aligned} \dot{z_1} &= z_2 \\ \dot{z_2} &= z_3 \\ \dot{z_3} &= z_4 \\ &. \\ \dot{z}_{n-1} &= z_n \\ \dot{z} &= v \end{aligned} \tag{21}$$

This proves that the resulting closed-loop system is linear and controllable. ■

The linearized state space model is thus given by

$$\begin{cases} \dot{z}_i = Az_i + Bv_i \\ y_{z_i} = Cz_i \end{cases} \quad \forall i \in \{1, 2, \ldots n\} \tag{22}$$

Where $A = \begin{bmatrix} 0 & 1 & 0 & . & . & 0 \\ 0 & 0 & 1 & . & . & 0 \\ . & . & . & . & . & . \\ . & . & . & . & . & . \\ 0 & 0 & 0 & . & . & 1 \\ 0 & 0 & 0 & . & . & 0 \end{bmatrix}_{nxn}$,

$B = \begin{bmatrix} 0 & 0 & 0 & . & . & 0 & 1 \end{bmatrix}^T_{nx1}$

$C = \begin{bmatrix} 1 & 0 & 0 & 0 & . & . & 0 \end{bmatrix}_{1xn}$

3.2 Adaptive and Cooperative Controller Design

In this section, the controller design following cooperative control algorithm having adaptive potential will be discussed separately for secondary control of AC microgrid not connected to main grid and distributed control of robotic agents in a mission of achieving a target. Figure 2 represents the schematic diagram of DG-based islanded AC microgrid, and Fig. 3 shows the distributed robots in a mission of achieving a target.

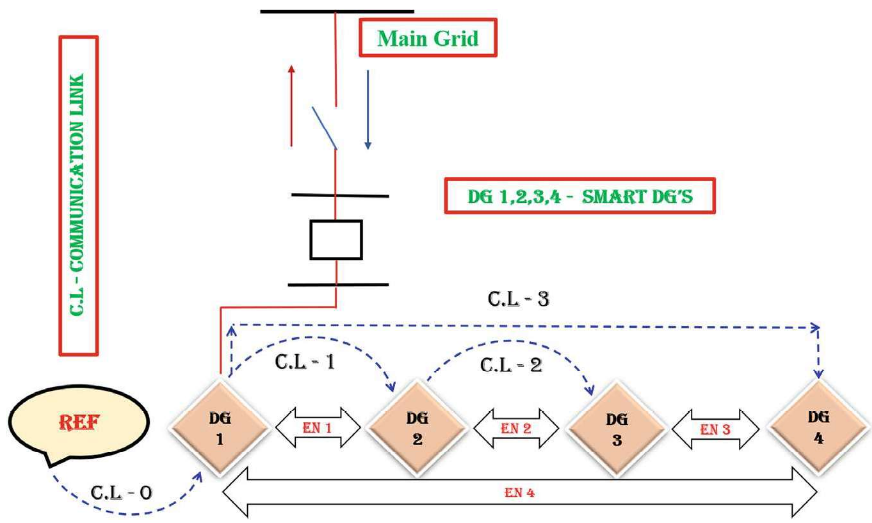

Fig. 2 Schematic diagram of a DG-based islanded AC microgrid

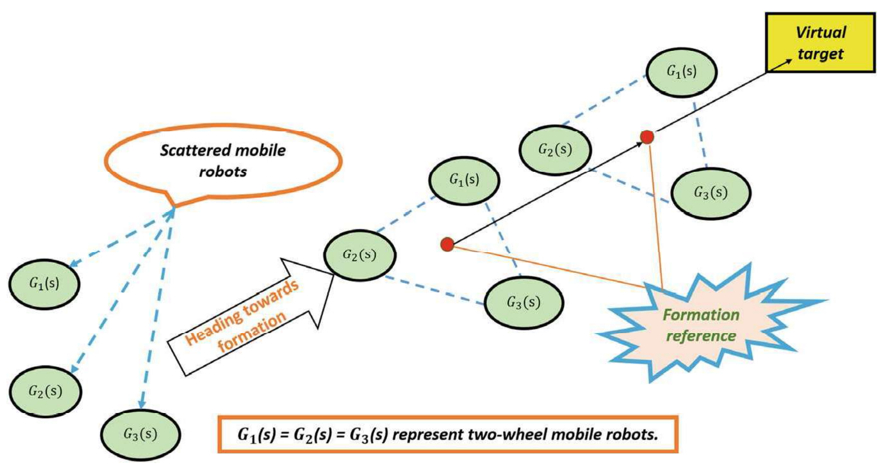

Fig. 3 Robotic agents in a mission

3.2.1 DG-Based Islanded AC Microgrid

This section discusses the de-centralized secondary adaptive voltage and frequency control scheme for an AC microgrid operating in islanded condition and consisting of N DG units. Using input-output feedback linearization, the linearized double integrator dynamics of the DG units for the design of secondary adaptive voltage controller is obtained as

$$\begin{cases} \dot{z}_i = Az_i + Bv_i \\ y_i = Cz_i \end{cases} \quad \forall i \in \{1, 2, \ldots \mathcal{N}\} \tag{23}$$

and the linearized single integrator dynamics for secondary adaptive frequency controller design is given by

$$\dot{\omega}_i = v_{fi} \qquad \forall i \in \{1, 2, \ldots \mathcal{N}\}. \tag{24}$$

Consider a spanning tree reflected through the adjacency matrix $\mathcal{A} = [a_{ij}]$ $\forall i, j \in \{1, 2, \ldots \mathcal{N}\}$ that exists in microgrid network having non-varying topology among the DG units. The dispersed generator units achieve perfect voltage and frequency consensus by the following proposed secondary adaptive voltage and adaptive frequency control algorithm.

Control Algorithm 1: Secondary adaptive voltage control

---

1 : Select $\mathcal{N}$ number of DG's in the microgrid.
2 : Select Positive definite matrices $Q_v = Q^T{}_v > 0$ & $R_v = R^T{}_v > 0$.
3 : Calculate positive definite matrix P_v from the ARE equation

$$A^\top P_v + P_v A + Q_v - P_v B R_v^{-1} B^\top P_v = 0. \tag{25}$$

4 : Find the value of controller gain $K_v = -R_v^{-1} B^\top P_v$.
5 : **for** each individual DG $i \in \{1, 2, \ldots, \mathcal{N}\}$ **do**
6 : Calculate cooperative tracking error (ξ_{vi}) from

$$\xi_{vi} = \sum_{j \in \mathcal{N}_i} a_{ij} \left(z_i - z_j\right) + g_i \left(z_i - z_0\right) \quad \forall i \in \{1, 2, \ldots, \mathcal{N}\} \tag{26}$$

where z_0 represents the reference voltage state, $g_i > 0$ becomes the pinning gain and $\mathcal{N}_i$ corresponds to the set of all neighbouring DGs of the ith DG unit.
7 : Determine adaptive coupling gain c_{vi} by integrating $\dot{c}_{vi} = \xi_{vi}^\top \Theta_v \xi_{vi}$ where $\Theta_v = P_v B R_v^{-1} B^\top P_v$.
8 : Calculate $\rho_{vi} = \xi_{vi}^\top P \xi_{vi}$.
9 : Find the DG control input v_{vi} from $v_{vi} = \nu_i K_v \xi_{vi}$ where $\nu_i = (c_{vi} + \rho_{vi})$.
end for
10 : Repeat step 6 to step 9 for all DG units in the microgrid.

Control Algorithm 2: Secondary adaptive frequency control

---

1 : Select $\mathcal{N}$ number of DG's in the microgrid.
2 : Select Positive definite matrices $Q_f = Q_f^T > 0$ & $R_f = R_f^T > 0$.
3 : Substituting Q_f, R_f in Eq. (25) and with proper values of A and B, calculate

solution P_f of ARE.
4 : Find the value of controller gain $K_f = -\sqrt{\frac{Q_f}{R_f}}$.
5 : **for** each individual DG $\quad i \in \{1, 2, \ldots, \mathcal{N}\}$ **do**
6 : Calculate cooperative tracking error (ξ_{fi}) from

$$\xi_{fi} = \sum_{j \in \mathcal{N}_i} a_{ij} \left(\omega_i - \omega_j\right) + g_i \left(\omega_i - \omega_0\right) \quad \forall i \in \{1, 2, \ldots, \mathcal{N}\} \tag{27}$$

where ω_0 represents the reference frequency state, $g_i > 0$ becomes the pinning gain and $\mathcal{N}_i$ corresponds to the set of all neighbouring DGs of the ith DG unit.
7 : Determine adaptive coupling gain c_{fi} by integrating $\dot{c}_{fi} = Q_f \, \xi_{fi}^2$.
8 : Calculate $\rho_{fi} = \sqrt{Q_f R_f} \, \xi_{fi}^2$.
9 : Find the DG control input $v_{fi} = (c_{fi} + \rho_{fi}) K_f \, \xi_{fi}$.
end for
10 : Repeat step 6 to step 9 for all DG units in the microgrid.

3.2.2 Robotic Agents in a Mission

Applying feedback linearization, the non-linear kinematic model of the two-wheeled mobile robot is transformed into a linear state-space model given by

$$\dot{x}_{r_i} = A x_{r_i} + B u_{r_i} \quad \text{and} \quad y_{r_i} = C x_{r_i} \qquad \forall i \in \{1, 2 \ldots n_r\} \tag{28}$$

where $x_{r_i} = \left[x_{xi} \; v_{r_{xi}} \; x_{yi} \; v_{r_{yi}}\right]^\top$, $u_{r_i} = \left[u_{r_{xi}} \; u_{r_{yi}}\right]^\top$. Consider a spanning tree characterized by the adjacency matrix $\mathcal{A} = [a_{ij}] \quad \forall i, j \in \{1, 2, \ldots n_r\}$ that connects the robotic agents in a robotic network team. The robots maintaining a formation vector $\mathbf{h}$ with respect to a formation reference track their desired target $\mathbf{r}(t)$ perfectly by the following cooperative control protocol

$$u_{r_i} = \sigma K \sum_{j=1}^{n_r} a_{ij} \big((y_{r_i} - h_i) - (y_{r_j} - h_j)\big) + g_i (y_{r_i} - h_i - r) \tag{29}$$

$\forall i \in \{1, 2, \ldots, n_r\}$ having controller gain K and for coupling gain σ.

4 Case Study

This section shows a particular case where AC microgrid works in an islanded condition and comprises of four DG units. The positive definite matrix Q, control effort

R, controller gain K, ARE solution P, and the reference voltage and frequency state for voltage and frequency controller design are given below.

4.1 Case 1: Voltage Controller Design in a DG-Based Islanded AC Microgrid

$Q_v = \begin{bmatrix} 915 & 0 \\ 0 & 1318 \end{bmatrix}$, $R_v = 0.1$ & reference voltage state $z_0 = \begin{bmatrix} z_{01} & z_{02} \end{bmatrix}$ where $z_{01} = 1$pu (1 pu = 430 V) and $z_{02} = 0$ pu.

$K_v = \begin{bmatrix} 95.65 & 115.63 \end{bmatrix}$ & $P_v = \begin{bmatrix} 1106.10 & 9.56 \\ 9.56 & 11.56 \end{bmatrix}$.

The voltage response of the DGs due to adaptive design of the microgrid secondary voltage controller of the considered AC microgrid disconnected to main grid is shown in Fig. 4 for the above-mentioned design parameters.

4.2 Case 2 : Frequency Controller Design in a DG-Based Islanded AC Microgrid

$Q_f = 150$, $R_f = 0.1$. $P_f = 3.87$ & $K_f = 38.72$. Reference frequency = 1 pu (1 pu = 50 Hz). Figure 5 shows the frequency response of the DGs due to adaptive design of the microgrid secondary frequency controller for the above-mentioned design parameters.

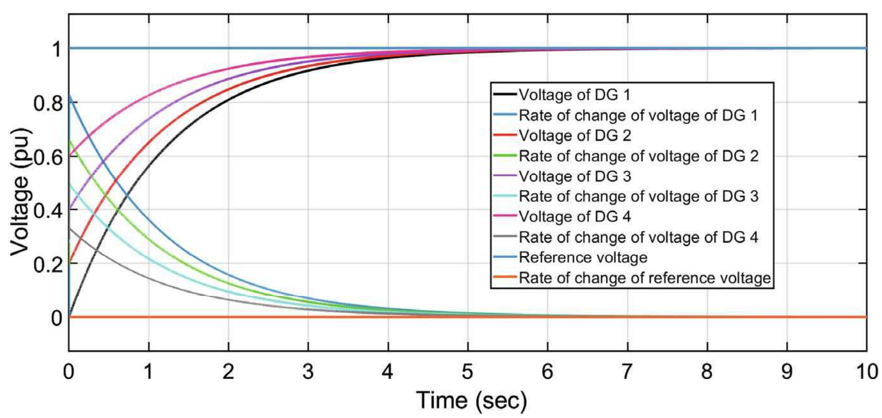

Fig. 4 Voltage response of the DGs due to adaptive design of the secondary voltage controller

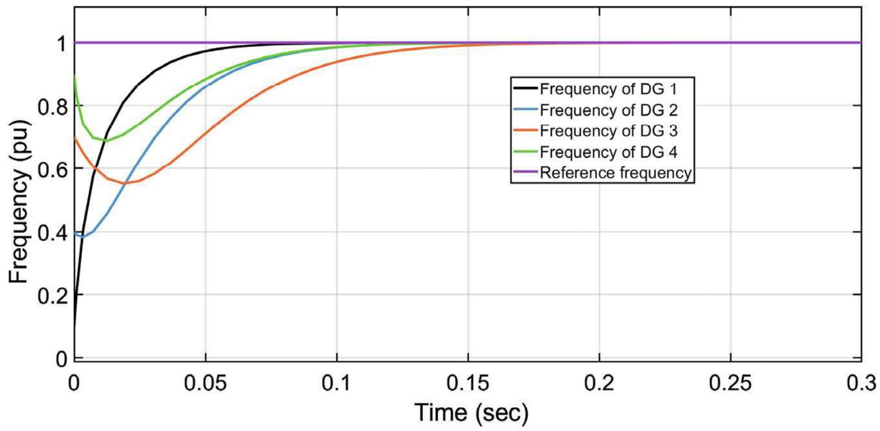

Fig. 5 Frequency profile of the DGs due to adaptive design of the secondary frequency controller

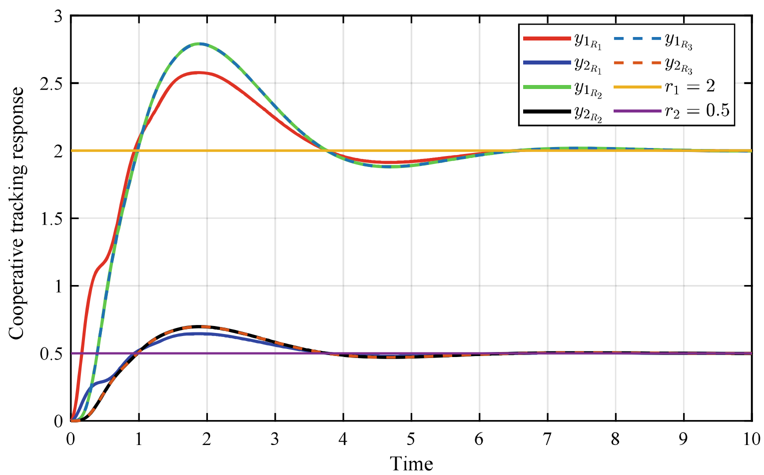

Fig. 6 Reference tracking following cooperative control scheme by three two-wheeled mobile robots

4.3 *Case 3 : Cooperative Control of Three Two-Wheel Mobile Robots*

Here, the team comprises of three two-wheel mobile robots having formation vector h = 0, which are connected through a particular network topology and aim to reach a particular target $\mathbf{r} = [r_1\ r_2]^\top = [2\ 0.5]^\top$. Figure 6 shows the states of three robots (R_1, R_2, R_3) tracking the reference following cooperative control protocol. The linearized robot models are represented by a decoupled double integrator system $M(s) = I_2 \otimes \frac{1}{s^2}$.

Table 2 Comparative analysis: adaptive versus conventional cooperative control algorithm of voltage controller

Time domain specifications	Adaptive control	Cooperative control
Rise time	2.65	4.75
Settling time	4.7	8.39
Overshoot percentage	0	0
Peak time	10	15

Table 3 Comparative analysis: adaptive versus conventional cooperative control algorithm of frequency controller

Time domain specifications	Adaptive control	Cooperative control
Rise time	0.058	0.15
Settling time	0.095	0.232
Overshoot percentage	0	0
Peak time	0.3	0.5

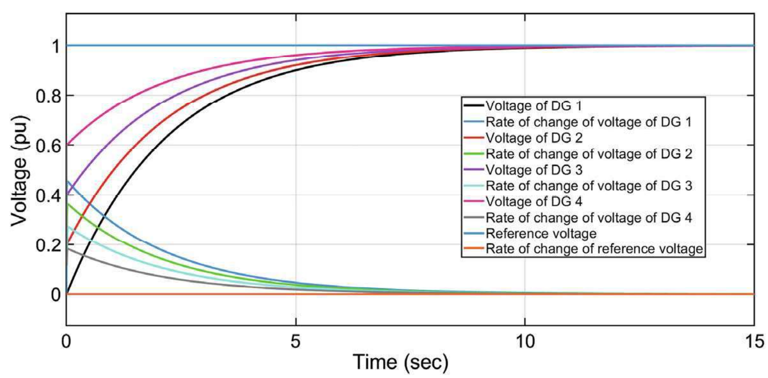

Fig. 7 Voltage response of the DGs due to cooperative design of the secondary voltage controller

The proposed adaptive control algorithm of the voltage and frequency controller of DG-based islanded AC microgrid has been compared with the standard conventional cooperative control algorithm [17]. The design of cooperative voltage controller demands the positive definite matrix $Q_v = \begin{bmatrix} 122 & 0 \\ 0 & 570 \end{bmatrix}$, control effort $R_v = 0.1$ and controller gain $K_v = \begin{bmatrix} 34.92 & 75.95 \end{bmatrix}$. The design parameters for cooperative frequency controller design are $Q_f = 3.7$, $R_f = 0.1$ and $K_f = 6.08$. Figures 7 and 8 show the cooperative voltage and frequency profile of DG-based islanded AC microgrid. The comparative analysis of the proposed adaptive control algorithm over the conventional cooperative control law in terms of some of the time domain specifications is presented in Tables 2 and 3.

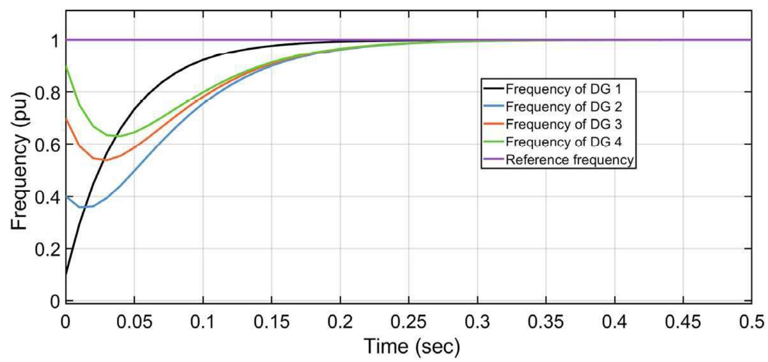

Fig. 8 Frequency response of the DGs due to cooperative design of the secondary frequency controller

4.4 Discussion

A fine controller tuning has been done for the adaptive controller having variable coupling gain and adaptive voltage and frequency profile of the microgrid are shown in Figs. 4 and 5. Figures 7 and 8 show the fine-tuned cooperative voltage and frequency profile of the considered microgrid network for the specified controller parameters. Some time domain specifications are given in Tables 2 and 3 for both the voltage and frequency profile obtained from both the mentioned controller designs. The data in Tables 2 and 3 clarify the comparative analysis of secondary adaptive and cooperative control schemes for the considered microgrid network.

5 Conclusion

In this work, the method of conversion of non-linear dynamics of the systems into their reformulated linearized forms using feedback linearization has been discussed in details. Input-output feedback linearization has been used to convert the non-linear dynamics into single and double integrator forms. These linearized forms enabled the application of adaptive and cooperative controller design in a multi-agent network. The multi-agent networks considered here are DG-based islanded AC microgrid and a team of robotic agents. Secondary controller design employing adaptive control algorithm has been done successfully for DG-based islanded AC microgrid comprising of four DGs. A comparative analysis done between the proposed adaptive control algorithm and the conventional cooperative control law demonstrates the effectiveness of the proposed adaptive control design of the microgrid secondary controller. Distributed cooperative controller design for achieving a target object has also become successful for a team of robotic agents comprising of three two-wheel mobile robots. In future, the objective is to design the gain of adaptive controllers using negative imaginary/strictly negative imaginary (NI/SNI) property [19] so as to ensure robust performance and to enhance robust stability of the interconnected systems.

References

1. Ogata K (2001) Modern control engineering, 4th edn. Prentice Hall PTR, USA
2. Naiborhu J, Firman F (2013) Output tracking of non-minimum phase nonlinear systems through exact linearization. Lect Notes Eng Comput Sci 2:988–991
3. Wang Y, Dong S, Ou L, Liu L (2015) Cooperative control of multi-missile systems. IET Control Theory Appl 9:441–446. https://doi.org/10.1049/iet-cta.2014.0361
4. Li J, Feng T, Zhang J, Yan F (2021) Optimal distributed cooperative control for multi-agent systems with constrains on convergence speed and control input. Neurocomputing 426:14–25. ISSN 0925-2312
5. Ren W, Beard RW (2008) Distributed consensus in multi-vehicle cooperative control, Berlin, Germany. Springer
6. Slotine JJE, Li W (2009) Applied nonlinear control. Prentice-Hall, Upper Saddle River, NJ, USA
7. Lewis FL, Syrmos VL (1995) Optimal control. Wiley, New York, NY, USA
8. Krumov AV (2005) Model and stability of a class of time-varying linear systems. In: EUROCON 2005—the international conference on computer as a tool, pp 1216–1219
9. Green RC, Wang L, Alam M (2013) Applications and trends of high performance computing for electric power systems: focusing on smart grid. IEEE Trans Smart Grid 4(2):922–931. https://doi.org/10.1109/TSG.2012.2225646
10. Wang D et al (2018) Review of key problems related to integrated energy distribution systems. CSEE J Power Energy Syst 4(2):130–145
11. Chromik JJ, Remke A, Haverkort BR (2016) What's under the hood? improving SCADA security with process awareness. In: 2016 joint workshop on cyber-physical security and resilience in smart grids (CPSR-SG), pp 1–6. https://doi.org/10.1109/CPSRSG.2016.7684100
12. Yang Z, Li Y, Xiang J (2019) Coordination control strategy for power management of active distribution networks. IEEE Trans Smart Grid 10(5):5524–5535
13. Murray RM (2007) Recent research in cooperative control of multivehicle systems. J Dyn Syst, Meas Control 129(5):571–583
14. Feng Y, Xu S, Zhang B (2014) Group consensus control for double integrator dynamic multiagent systems with fixed communication topology. Int J Robust Nonlinear Control 24(3):532–547
15. Sepulchre R, Paley D, Leonard N (2005) Collective motion and oscillator synchronization. Springer Berlin Heidelberg, Berlin, Heidelberg, pp 189–205
16. Horn RA, Johnson CR (2012) Matrix analysis, 2nd edn. Cambridge University Press, New York, USA
17. Olfati-Saber R, Fax JA, Murray RM (2007) Consensus and cooperation in networked multi-agent systems. Proc IEEE 95(1):215–233
18. Fax JA, Murray RM (2004) Information flow and cooperative control of vehicle formations. IEEE Trans Autom Control 49(9):1465–1476
19. Bhowmick P, Lanzon A (2021) Applying negative imaginary systems theory to non-square systems with polytopic uncertainty. Automatica 128:109570(1–18)